UDC 629.765
Doi: 10.31772/2712-8970-2024-25-2-233-246

Для цитирования: Кольга В. В., Рундау Н. С. Исследование параметров движения входа космоплана в атмосферу // Сибирский аэрокосмический журнал. 2024. Т. 25, № 2. С. 233–246. Doi: 10.31772/2712-8970-2024-25-2-233-246.

For citation: Kolga V. V., Runda N. S. [Research of the motion parameters of a spaceplane entry of into the atmosphere]. *Siberian Aerospace Journal.* 2024, Vol. 25, No. 2, P. 233–246. Doi: 10.31772/2712-8970-2024-25-2-233-246.

Исследование параметров движения входа космоплана в атмосферу

В. В. Кольга*, Н. С. Рундау

Сибирский государственный университет науки и технологий имени академика М. Ф. Решетнева
Российская Федерация, 660037, г. Красноярск, просп. им. газ. «Красноярский рабочий», 31
*E-mail: kolgavv@yandex.ru

После прекращения эксплуатации Международной космической станции в 2028 г., Российская Федерация планирует развивать проект национальной орбитальной станции. Российская орбитальная станция будет отличаться от своего предшественника большей практической направленностью. Одной из задач, возлагаемых на станцию, является запуск и управление группировки малых спутников дистанционного зондирования Земли, а также взаимодействие и обслуживание перспективных спутниковых группировок. Так как возможности маневрирования орбитальной станции весьма ограничены, а неисправный аппарат может находиться в значительном удалении от неё, то для повышения транспортно-технических возможностей станции предлагается использовать беспилотный космоплан.

В работе представлены два аэродинамических облика космоплана, в результате аэродинамического и весового анализов которых был сделан выбор в пользу первого, описаны компоновка аппарата и алгоритмы его работы на орбите и спуске в атмосферу.

Целью исследования является сравнение параметров траектории при спуске аппарата с различных орбит схода. Для этого сформулирована задача по определению зависимости площади коридора входа от начальных параметров. В свою очередь, площадь коридора входа определялась граничными условиями, зависящими от эксплуатационных параметров космоплана.

Для определения параметров входа написана расчётная программа, решающая дифференциальные уравнения движения летательного аппарата методом Эйлера в общем случае и методом Рунге – Кутта в расчётном случае.

В качестве результатов исследования представлена зависимость площади коридора входа от высоты орбиты схода, а также графические зависимости основных параметров для расчётного случая.

Ключевые слова: космоплан, Российская орбитальная станция, движение в плотных слоях атмосферы, траектория, алгоритм функционирования.

Research of the motion parameters of a spaceplane entry into the atmosphere

V. V. Kolga*, N. S. Rundau

Reshetnev Siberian State University of Science and Technology
31, Krasnoyarskii rabochii prospekt, Krasnoyarsk, 660037, Russian Federation
*E-mail: kolgavv@yandex.ru

After cessation of operation of the International Space Station in 2028, the Russian Federation plans to develop a national orbital station project. The Russian Space Station will differ from its predecessor in a greater practical aspect. One of the tasks assigned to the station will be the launch and management of a group of small satellites for remote sensing of the Earth, as well as the interaction and maintenance of prospective satellite groups. Due to the limited maneuverability of the orbital station and the potential for a malfunctioning device to be at a significant distance from it, the use of an autonomous spaceplane is proposed to increase the transportation and technical capabilities of the station.

The research presents two aerodynamic designs of the spaceplane, and one of them is chosen based on the results of the aerodynamic and weight analysis. The spaceplane configuration and algorithms for its operation on the orbit and descent to the atmosphere are also presented. The goal of the research is to compare the trajectory parameters during the descent of the spacecraft from different descent orbits. For this purpose, a task was specified to determine the dependence of the area of the descent corridor on the initial parameters. The area of the descent corridor is determined by the boundary conditions, which depend on the operational parameters of the spaceplane. A computational program is written to solve differential equations of flight dynamics of a spaceplane by Euler's method in general and by Runge-Kutta method in a computational case. The results of the research are presented as the dependence of the area of the descent corridor on the altitude of descent. Graphical representations of the primary parameters of the spaceplane descent for the computational case are also provided.

Keywords: spaceplane, Russian Orbital Station, movement in dense layers of the atmosphere, trajectory, algorithm of functioning.

Introduction

After the cessation of operation of the International Space Station (ISS) in 2028, the Russian Federation plans to develop a national orbital station project. The Russian orbital station (ROS) will differ from its predecessor in being more practical. For this purpose, the ROS will be placed in orbits above 250 km with an inclination of 98°, which will allow it to:

– control the ice situation on the Northern Sea Route, Antarctica and the waters of the World Ocean;

– monitor the environmental situation in the territory of the Russian Federation;

– monitor the ionosphere, climate and microphysical processes;

– explore the Earth's magnetic field;

– register the disturbances in the Earth’s atmosphere within the given timeframe [1].

In addition, the ROS (Fig. 1) is assigned to launch and manage a constellation of small satellites for remote sensing of the Earth, as well as interaction and maintenance of promising satellite constellations [1].

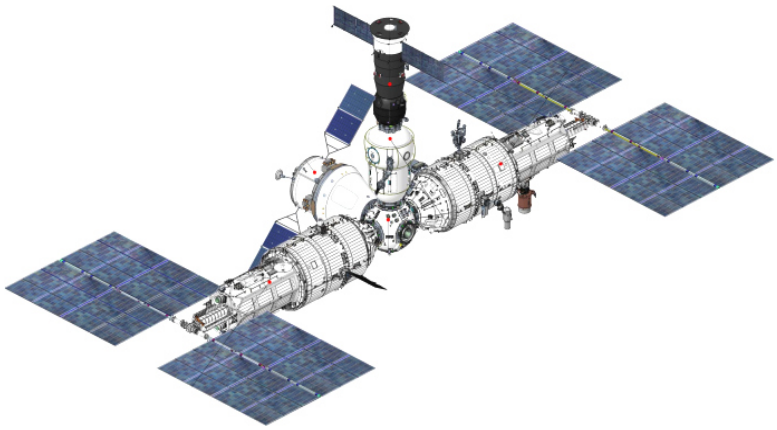

Рис. 1. Российская орбитальная станция

Fig. 1. The Russian Orbital Station

Since the maneuvering capabilities of the orbital station are very limited, and a faulty vehicle may be located at a considerable distance from it, it is proposed to use an unmanned spaceplane to increase the transport and technical capabilities of the ROS. This type of device is a glider that has a full set of aerodynamic controls in addition to standard gas-dynamic ones and has a hypersonic lift-to-drag coefficient greater than one. The spaceplane obtains the following number of advantages:

– the vehicle is capable of covering a wide range of orbits due to the presence of a more developed propulsion system (PS) compared to satellites and orbital stations;

– the reusability of the spaceplane, combined with a low load factor at the atmospheric reentry site, makes it possible to deliver to Earth for repair both individual faulty satellite elements and entire small-sized vehicles;

– the vehicle significantly saves financial resources, as it allows to solve problems with fewer targeted funds;

– the spaceplane allows to reduce financial resources for search and rescue operations due to landing at the airfield “like an airplane”;

– the vehicles’ multitasking nature permits it to be used as a platform for organizing research activities and testing technologies under the conditions close to deep space [2].

This research task was set to design a spaceplane for transport and technical support of a promising orbital station. To realize the task, an analysis of the aerodynamic configurations of such vehicles was carried out, an algorithm for the operation of the device was developed, and the parameters of entry into the atmosphere were determined taking into account the boundary conditions.

Aerodynamic configuration № 1

The model was constructed using the cross-sectional method with a set of spatial curve guides, using the external appearance of the X-37B apparatus as the source material [3].

Figure 2 demonstrates the resulting aerodynamic configuration № 1

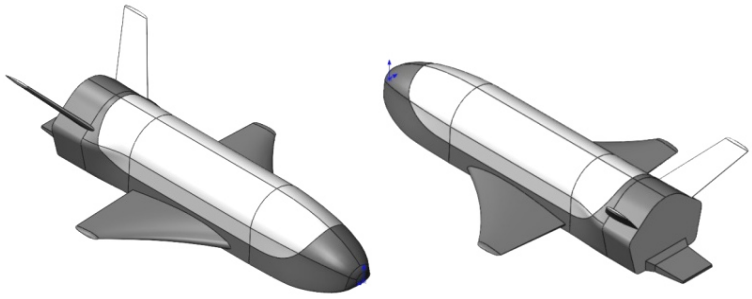

Рис. 2. Аэродинамическая компоновка № 1

Fig. 2. Aerodynamic configuration No. 1

This geometric appearance is made according to the “normal” balancing scheme with a low-mounted wing of the “ogival delta” type and a V-shaped empannage.

The elongated fuselage provides a high aerodynamic quality index, has a massive nose blunting to form the strongest shock waves during hypersonic flow, which reduces thermal loads on the surface of the vehicle, and a pronounced widening in the aft section forms a shaded area for the vertical empennage when entering the atmosphere [4].

The selected “ogival delta” configuration provides increased lift at high angles of attack, and the positive V-angle provides increased lateral stability of the orbital aircraft. The wing is set relative to the course with a zero angle of attack [5].

At atmospheric entry points, the selected V-shaped empennage, due to the ability to control three channels at once, provides increased maneuverability characteristics and also forms a streamlined profile of the aircraft at high angles of attack.

With this balancing scheme, the aircraft is controlled using three main aerodynamic planes: the balancing flap, the vertical empennage and the ailerons.

Balancing and setting the required angle of attack in atmosphere dense layers during hypersonic movement is performed using an aerodynamic (balancing) flap. Control via the yaw and roll channels is carried out by means of the combined deflection of the two vertical stabilizer fins; pitch control in the late stages of atmospheric flight, in turn, is realized by means of their differential deflection; control via the roll channels is realized by means of differential deflection of the ailerons. The combined deflection of the ailerons provides the vehicle with the necessary lifting force at the moment of landing [5].

After constructing a 3D model of the spaceplane, an approximate aerodynamic study was conducted in SolidWorks CAD, resulting is the law of change in aerodynamic quality due to the Mach number:

$$K = 2,0005 \cdot M^{-0,179}. \quad (1)$$

Further, a weight analysis was performed in the first approximation using the relative masses of similar vehicles, considering the form factor of the aerodynamic configuration. The results of the weight analysis are presented in Table 1 [6].

Table 1

Weight analysis results of aerodynamic configuration No. 1

	Vehicle dry weight	Vehicle launch mass	Fuel mass (UDMH)	Oxidizer mass (AT)
Parameter value, kg	4450	12400	2115	4335

Aerodynamic configuration № 2

The model was constructed using the “section” method with a set of spatial guide curves; the HL-20A1 variant [7] was taken as the initial data for constructing the 3D model of the apparatus.

Fig.3 demonstrates the resulting aerodynamic concept of FD-2.

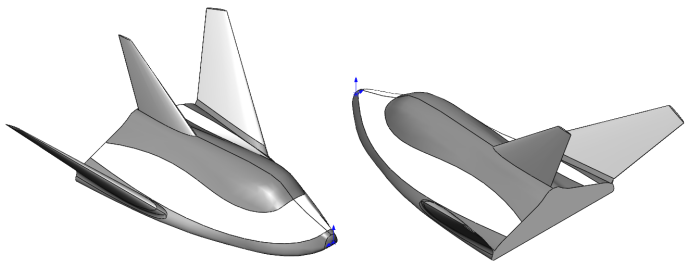

Рис. 3. Аэродинамическая компоновка № 2

Fig. 3. Aerodynamic configuration No. 2

FD-2 glider is designed using a “lifting body” aerodynamic configuration with additional swept wing consoles installed at an angle of 44.65°, as well as a keel installed in the aft part of the aircraft.

The fuselage of this shape provides high flight characteristics due to the large aerodynamic surface, and also creates a massive shadow area with lower thermal loads in the upper part of the apparatus. The overall blunt profile forms the strongest shock waves during hypersonic flow, which reduces thermal loads on the surface of the vehicle as a whole [4].

Two additional wing consoles increase the aerodynamic quality of the aircraft, due to the increase in aerodynamic surfaces, and also contribute to its self-balancing at the required angles of attack equal to 30 to 45°, due to the pre-selected angle of positive V installation. The sweep of the additional consoles reduces drag, which also improves the aerodynamic quality of the vehicle. The sweep angle at the leading edge is 55°. The vertical empennage keel ensures the directional stability of the aircraft during the atmospheric portion of the flight. The keel sweep is 52° [8].

Control of the vehicle with this aerodynamic concept is carried out using three main aerodynamic planes: the balancing flap, the vertical empennage and the elevons. Balancing and setting the required angle of attack in “non-self-balancing” modes are carried out using an aerodynamic flap. Control through the pitch and roll channels is done using the joint deflection of two elevons of the additional wing consoles; pitch control in late atmospheric stages, in turn, is performed using their differential deviation. To control the yaw channel, the rudder is used in the vertical direction.

After constructing a 3D model of the spaceplane, an approximate aerodynamic study was carried out in the SolidWorks CAD system, resulting in the law of change in aerodynamic quality from the Mach number:

$$K = 2{,}3344 \cdot M^{-0{,}215}. \quad (2)$$

Further, a weight analysis was carried out to a first approximation using the relative masses of similar devices, taking into account the form factor of the aerodynamic configuration. Table 2 demonstrates the results of the weight analysis [6].

Table 2

Weight analysis results of aerodynamic configuration No. 2

	Vehicle dry weight	Vehicle launch mass	Fuel mass (UDMH)	Oxidizer mass (AT)
Parameter value, kg	4450	8760	1415	2895

Choosing the final concept of the future spaceplane

The choice of the future spaceplane concept is determined by the following basic parameters:

– mass characteristics;
– energy characteristics;
– aerodynamic characteristics;
– overall parameters;
– manufacturing complexity.

According to the results of the weight analysis, the vehicle with aerodynamic configuration No. 2 turned out to be 3640 kg lighter than with aerodynamic configuration No. 1. This is explained by the significantly lower capacity of the fuel tanks of configuration No. 1, due to the more complex shape of the fuselage in the aft and middle parts. Figure 4 presents internal configuration of the two aerodynamic concepts.

The vehicle with aerodynamic concept No. 1 has larger fuel tanks compared to No. 2, which allows it to cover a significantly larger range of orbits, thereby significantly increasing the transport and technical capabilities of the ROS.

The aerodynamic characteristics of concept No. 2, according to the results of calculating the determination of the aerodynamic quality, turned out to be 5% higher, this is explained by the larger wing area, and the insignificant increase is due to the smaller elongation of the fuselage.

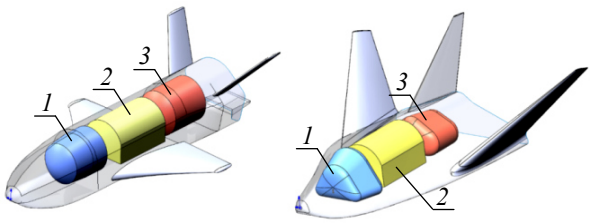

Рис. 4. Компоновка топливных отсеков обоих аэродинамических обликов:
1 – бак горючего; *2* – полезный груз; *3* – бак окислителя

Fig. 4. Configuration of the fuel compartments of both aerodynamic concepts:
1 – fuel tank; *2* – payload; *3* – oxidizer tank

Aerodynamic configuration No. 2 has large overall dimensions in height and width, inferior to concept) No. 1 only in length, which makes it more difficult to fit under the nose fairing halves of the carrier-vehicle. The less stable shape of the aft part prevents the placing shape No. 2 on standard type adapters, which forces the use of a specialized bed.

Both aerodynamic models have a complex airframe design, but model No. 2, due to the specific shape of the fuselage, is equipped with profiled fuel tanks, which significantly complicates the assembly technology of the final aircraft.

Summarizing all of the above, the choice has been made in favor of aerodynamic configuration No. 1, since this scheme has high energy parameters combined with good aerodynamic qualities, acceptable overall dimensions that allow it to be placed under the head fairings of existing rockets, and fuel tanks that are easier to manufacture.

Algorithm for a spaceplane functioning in the orbit

The spaceplane work cycle under the program of towing a malfanctioning satellite consists of the six main stages presented in Fig. 5.

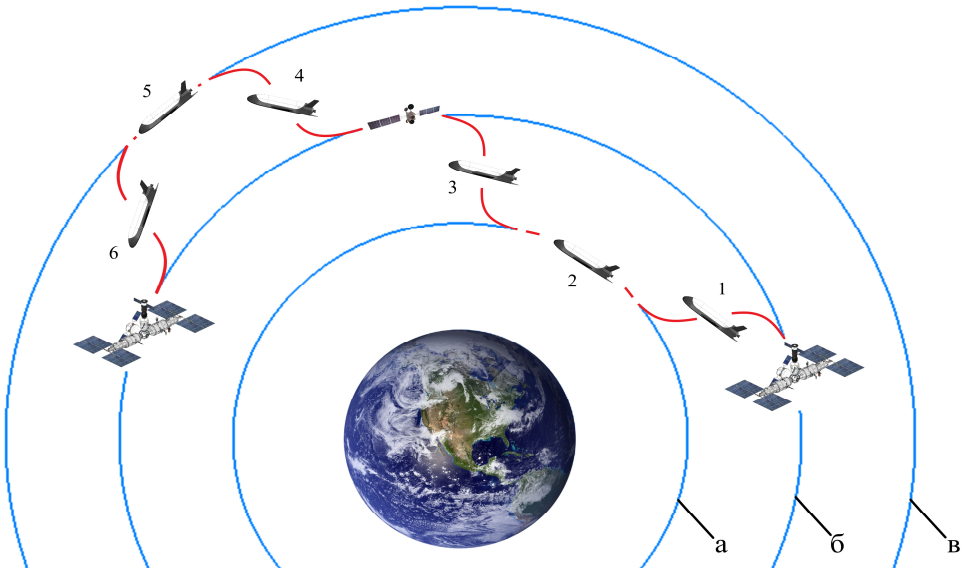

Рис. 5. Рабочий цикл космоплана

Fig. 5. Spaceplane duty cycle

1. *Transfer to orbit "a".* Having received a flight mission, the spaceplane undocks from the ROS. The on-board digital computing complex (ONDC) determines the parameters of the elliptical transfer orbit and the magnitude of two pulses. Further, with the help of correction engines (CE), the vehicle is guided, and the main propulsion system implements the first impulse at the apogee and the second impulse after re-guiding at the perigee of the transfer orbit.

2. Phasing for rendezvous with a malfanctioning satellite. After transition to orbit "a", the on-board center determines the phasing time for transition to the area where the malfanctioning satellite is located. Minimization of phasing time is achieved by a higher orbital speed, since orbit "a" is significantly lower than orbit "б".

3. Transfer to orbit "б" and capture of a faulty satellite. After the phasing time has expired, the spaceplane's ONDC makes transitions along an elliptical orbit. The CEs deploy the spaceplane along the course of movement, and the main propulsion system implements the first impulse at the perigee of the transfer orbit. Next, a turn occurs with the CE help and the second braking impulse is realized at the apogee of the elliptical orbit. After completing the transition, a sighting device extends from the cargo compartment to detect the device, and a manipulator arm also deploys to capture the damaged vehicle.

4. *Transfer to orbit "в".* Having captured the satellite and placed it in the cargo bay, the ONDC begins calculating the parameters of the transition to orbit "б", after which a transition similar to that described in paragraph 3 is implemented.

5. Phasing for approaching the ROS. After transition to orbit "b", the ONDC determines the phasing time for transition to the orbital region where the ROS is located. Minimization of phasing time is achieved by a lower orbital speed, since orbit "в" is located significantly higher than orbit "б".

6. Transfer to orbit "б" and docking with ROS. Further, the spaceplane with the damaged satellite makes the transition according to an algorithm similar to point 1. After the transition is completed, the spaceplane performs a docking maneuver to the orbital station

Spaceplane design

Based on the aerodynamic concept, a layout diagram of the spaceplane was designed, shown in Fig. 6. The basis of the spaceplane design is the glider. It forms aerodynamic contours, absorbs loads in all phases of flight, serves the spacecraft body and includes systems and elements that ensure descent and landing. Due to the design, the glider can be divided into several main parts:

– nose fuselage;
– mid fuselage;
– aft body;
– two wing consoles.

Each of the above elements consists of a spar-frame set reinforced by a shell.

The layout of the spaceplane includes the following main elements and systems:

– bow (1) and stern (8) correction engine(CE) blocks;
– on-board digital computing complex (ONDC) with a battery(*2*);
– sighting device (*3*);
– manipulator arm (*4*);
– fuel system (*5*);
– basic propulsion system (*7*);
– electric drives of aerodynamic control (*6*).

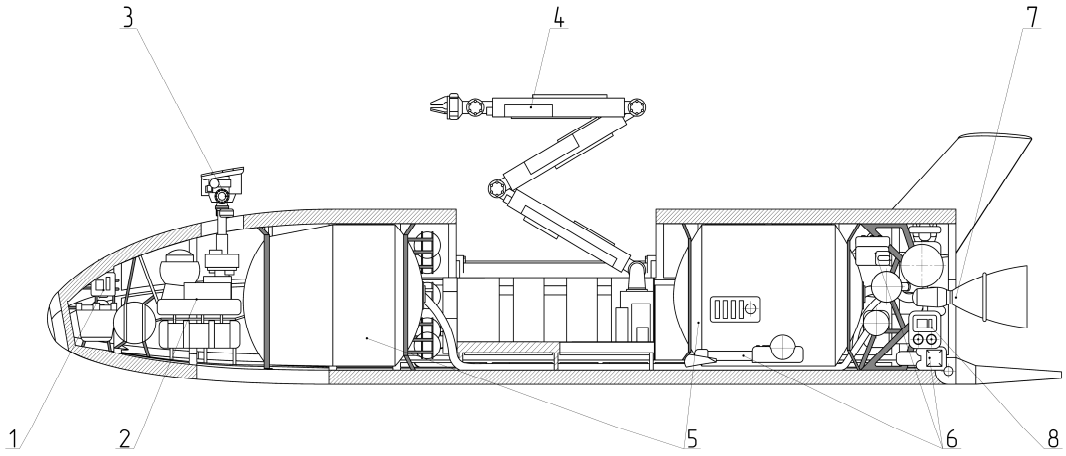

Рис. 6. Компоновочная схема космоплана:
1 – носовой блок двигателей коррекции; *2* – БЦВК с аккумуляторной батареей;
3 – визирующее устройство; *4* – рука-манипулятор; *5* – топливная система; *6* – электроприводы аэродинамических органов управления; *7* – маршевая силовая установка;
8 – кормовой блок двигателей коррекции

Fig. 6. Spaceplane layout diagram:
1 – bow block of correction engines; *2* – on-board digital computing complex (ONDC) with a battery;
3 – sighting device; *4* – manipulator arm; *5* – fuel system; *6* – electric drives of aerodynamic control; *7* – basic propulsion system; *8* – aft block of correction engines

CE blocks are designed to control the spaceplane outside atmospheric areas. They are represented by bow and stern units, combinations of inclusions of which provide control over all three channels: yaw, pitch and roll. CE units are powered by locally located small fuel tanks of the displacement supply system [9].

The ONDC with a battery is located in the bow of the vehicle. Two rechargeable batteries provide operation of the on-board electrical network and the main computer. The batteries are recharged from the orbital station or solar panels installed on the cargo compartment doors. The on-board computer itself is represented by four main blocks with equal delegation of the main spaceplane systems and two backup ones.

The sighting device is installed in a hinged suspension, which provides full visibility in the upper hemisphere of the spaceplane, on a telescopic rod. The device itself consists of two telescopic cameras in the light and thermal range and a laser rangefinder. The sighting device is protected by a ceramic panel on the top acting as a hatch cover.

The manipulator arm consists of three movable joints that provide capture of the satellite at a distance of up to 5 m from the spaceplane, and articulated units in the elbows of the device allow for capture in the upper hemisphere of the vehicle. The base of the manipulator is rigidly fixed in the cargo compartment of the orbital aircraft, and the control computer is also located there [10].

The fuel system is represented by two main oxidizer and fuel tanks and four small ones located in the bow and stern parts of the vehicle. Small tanks are powered from the main tanks by an electric pump, thereby forming a power supply system for the CE units.Using the main lines, fuel is supplied to the main propulsion system. To implement fuel intake in all flight modes, both “rocket” (funnel suppressor on the bottom of the tank) and “aircraft” (through a system of intakes on the shell) fuel intake are provided.

The basic propulsion system is represented by the C5.92 engine, rigidly mounted in the frame. Power is provided using a turbocharged unit, the exhaust gas of which is thrown overboard the spaceplane [11].

Electric drives of the aerodynamic controls provide control of the vehicle in the atmospheric section. They are represented by two electric drives for deflecting the ailerons, two electric drives for deflecting the rudders and one high-power electric drive for deflecting the balancing flap.

Atmosphere entry procedure

After completing a mission, the spaceplane begins its descent into the atmosphere. Before the start of descent, the spaceplane in orbit “A” makes a turn against the movement for the subsequent implementation of the braking impulse. The entry into the atmosphere itself consists of 4 main stages, shown in Fig. 7 [12].

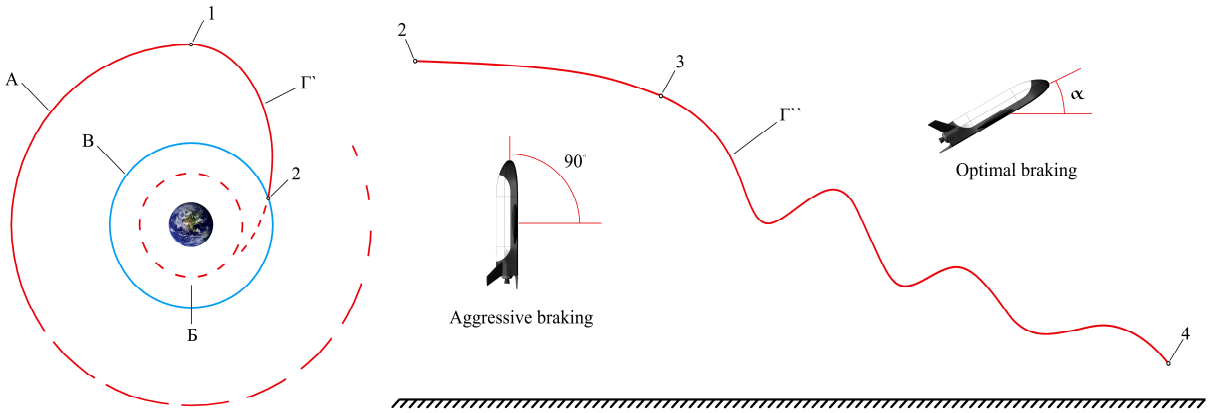

Рис. 7. Траектория входа в атмосферу

Fig. 7. Atmospheric entry trajectory

1. Transition to the descent trajectory. At point *1* of the descent orbit “А”, having previously determined the landing area on the Earth’s surface, a braking impulse is carried out and a transfer elliptical orbit “Г`” is formed, which is an extra-atmospheric section of the entry trajectory. The transition is made to an imaginary circular orbit “Б”, the altitude of which is selected to guarantee sufficient time for the spaceplane to remain in the atmosphere to ensure landing.

2. Entry into the atmosphere. At point 2, the vehicle enters the planet’s atmosphere (the atmosphere is indicated by “В”). Immediately after entry, an “aggressive” braking maneuver occurs, the essence of which is that the device sets an angle of attack equal to 90°. The angle is set using the bow and stern CE blocks. As a result of this maneuver, the elliptical trajectory “Г`” under the influence of drag forces is modified to the descending branch of a parabola.

3. Movement along a wave-like trajectory. At point 3, the “aggressive” braking maneuver is completed and the angle of attack is set, ensuring maximum aerodynamic quality at the corresponding Mach number. The setting itself is carried out using aerodynamic controls. As a result of the combined action of drag and lift forces, the trajectory is deformed to a wavy descending curve.

4. Completion of the ballistic section of the descent. At an altitude of 20 km above the Earth's surface, the spaceplane, impulsively launching the propulsion system, goes into horizontal flight and, gradually dropping the altitude and remaining speed, heads to the landing airfield.

Statement of the analysis problem

To carry out calculations within the framework of the second approximation, it is necessary to analyze the spaceplane entry trajectories in order to obtain temperature flow parameters and overload values at each moment of time that satisfy the operating conditions [13].

The descent trajectory for each mission is individual and is determined by parameters (location of the landing airfield, weather conditions, and others), which are not possible to take into account, but it is possible to set the parameters of the entry corridor. Boundary trajectories are determined by the operational and strength parameters of the spaceplane, such as maximum overload and maximum thermal load [8].

The maximum possible thermal load on the shell of the descent vehicle is realized during a rebound flight path, when the spaceplane leaves the planet atmosphere several times and returns to it again. During such a flight, due to the small dissipation of thermal energy in outer space, the aircraft remains in an overheated state for a long time. Therefore, as boundary conditions for the temperature load, we will take the first trajectory, in which the vehicle does not leave the Earth’s atmosphere. In other words, the height of the peak of the first wave should not exceed 100 km. This is achieved through short-term “aggressive” braking, the time of which will be minimal within the framework of this task and as a result of which, for a given trajectory, the maximum orthodromic range will be realized [8].

We are considering the maximum overload value at the atmospheric reentry site to be 1.9. This is explained by the presence in the cargo compartment of the evacuated satellite, which was not secured according to its operating instructions. This overload is achieved by long-term “aggressive” braking, the time of which will be the maximum in this task. Also, due to the duration of “aggressive” braking, a minimum orthodromic range will be realized with this trajectory.

Figure 8 presents the resulting visualization of the entry trajectory. The size of this corridor is characterized by the area $S_{к.вх}$, which completely depends on V_0 and θ_0 at the point of entry into the atmosphere. The parameters at the entry point, in turn, are determined by the trajectory of the extra-atmospheric section Г`, which completely depends on the value of the descent orbit “А”.

Therefore, summing up all of the above, the purpose of this analysis is to determine the dependence of the area of the entrance corridor $S_{к.вх}$ on the value of the descent orbit "A".

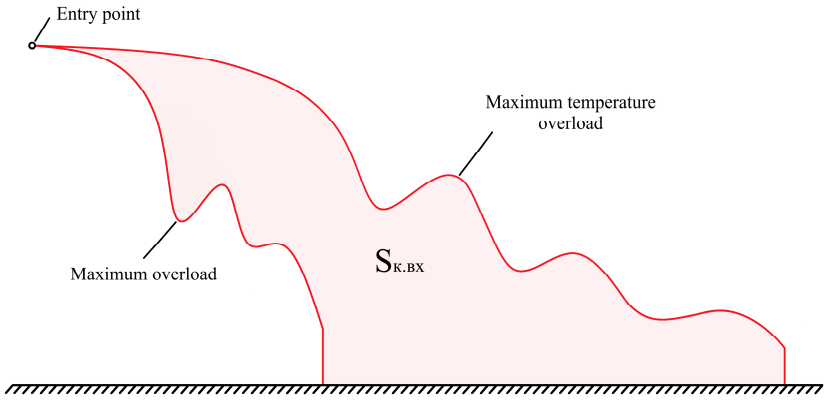

Рис. 8. Схема коридора входа

Fig. 8. Diagram of the entrance corridor

Solution to the reentry problem

The research studied a range of descent orbits with altitude values of 150–500 km with a step of 50 km. The altitude of entry into the atmosphere, as well as the conventional boundary of the atmosphere itself, was equal to100 km, and therefore, the atmospheric parameters were starting from this value [14]. The differential equations of motion for the problem solved are below [15]:

$$m\frac{dv}{dt} = -X_a - G\sin\theta, \tag{3}$$

$$mv\frac{d\theta}{dt} = Y_a - G\cos\theta + \frac{mv^2}{R_3 + H}\cos\theta. \tag{4}$$

The solution for the selected orbits was carried out in the Maple computer mathematics system using the Euler method, the general implementation of the method is presented in the form of the following equation [15]:

$$y_k = y_{k-1} + hy'_{k-1}, \tag{5}$$

where $y'_{k-1} = f\left(x_{k-1}, y_{k-1}\right)$.

The following initial conditions were accepted as the design case: descent orbit altitude $H_{орб}$ = 300 km, "aggressive" braking time t = 370 s. Differential equations are presented in formulae (3) and (4).

The solution for the chosen trajectory was performed in the Maple computer mathematics system using the Runge–Kutta method, the general implementation of the method is presented in the form of the following equation [15]:

$$\Delta y = \frac{h}{6}\left(y'_A + 2\left(y'_B + y'_C\right) + y'_D\right), \tag{6}$$

where

$$y'_A = f\left(x_A, y_A\right);$$

$$y_B^{'} = f\left(x_A + \frac{h}{2}, y_A + y_A^{'}\frac{h}{2}\right);$$

$$y_C^{'} = f\left(x_A + \frac{h}{2}, y_A + y_B^{'}\frac{h}{2}\right);$$

$$y_D^{'} = f\left(x_A + h, y_A + y_C^{'}h\right).$$

The temperature of the nose cone was determined by solving the following equation for $T_{\text{п.р}}$ [15]:

$$\varepsilon\sigma T_{\text{п.р}}^4 + \alpha T_{\text{п.р}} - \alpha T^* = 0, \quad (7)$$

where ε – effective emittance; σ – emissivity for an absolute black body; α – heat transfer ratio; T^* – representative temperature.

Calculation results

The obtained area values from various rendezvous orbits are summarized in Table. 3, the dependence of the area on the descent orbit is also shown in the form of a graph (Fig. 9).

Table 3

Results of calculating the corridor area from various rendezvous orbits

$H_{\text{орб}}$, km	150	200	250	300	350	400	450	500
$S_{\text{к.вх}}$, km^2	192206	184004	168875	169286	155478	157247	154654	147724

The results of the parameters for the design case (H_{orb} = 300 km, t = 370 s) are presented in the form of graphical dependencies (Fig. 10).

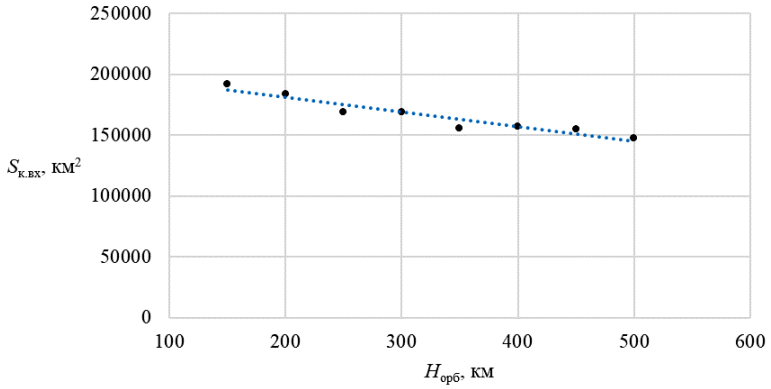

Рис. 9. График зависимости площади коридора от орбиты схода

Fig. 9. Dependency graph of the corridor area on the descent orbit

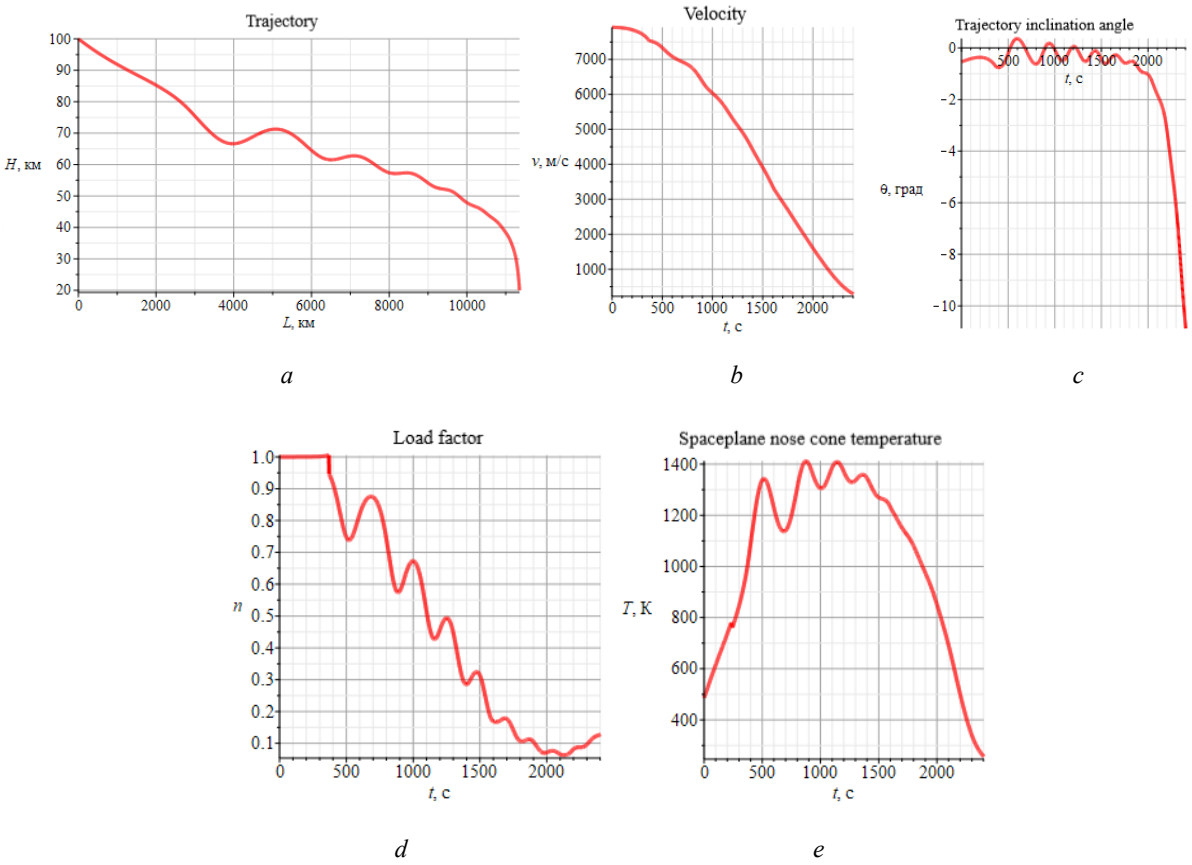

Рис. 10. Графики зависимостей:
a – высоты от ортодромной дальности; *b* – скорости от времени; *c* – угла наклона траектории от времени; *d* – коэффициента перегрузки от времени; *e* – температуры носового обтекателя от времени

Fig. 10. Dependency graphs:
a – height from the orthodromic range; *б* – velocity versus time; *в* – trajectory inclination angle from time; *г* – load factor from time; *д* – spaceplane nose cone temperature versus time

Conclusion

The research examined two aerodynamic configurations of an orbital aircraft, carried out their aerodynamic and weight analysis, based on the results of which a choice was made in favor of the first aerodynamic configuration. The internal layout of the orbital aircraft was designed, and an algorithm for functioning in the orbit and in the atmosphere was developed.

The solution of differential equations of motion in the atmosphere in the Maple computer algebra environment was implemented using the Euler method. The result of this decision is the entry corridor areas for various descent orbits, and, consequently, a variety of working trajectories for the descent of the spaceplane.

As a design case, we considered one of the possible trajectories with a descent orbit of 300 km and an “aggressive” braking time of 370 s. The solution to the design case was implemented by the Runge–Kutta method. Based on the results of solving the program, graphical dependences of the kinematic, dynamic and temperature parameters of the orbital aircraft on the atmospheric portion of the movement were obtained.

Библиографические ссылки

1. Соловьёв В. А. Развитие пилотируемой программы космических полётов на Российской Орбитальной Станции // XLVIII Академические чтения по космонавтике, посвященные памяти академика С. П. Королёва и других выдающихся отечественных ученых – пионеров освоения космического пространства (23–26 января). Москва, 2024.

2. Буран РУ [Электронный ресурс]. URL: http://buran.ru/htm/maxmain.htm (дата обращения: 13.02.2024).

3. Arthur C. Grantz X-37B Orbital Test Vehicle and Derivatives // AIAA SPACE 2011 Conference & Exposition. California, 2011. 14 p.

4. Лох У. Динамика и термодинамика спуска в атмосфере планет / пер. с англ. Е. А. Голякова и др. М. : Мир, 1966. 276 с.

5. Lyndon B. J. Space Shuttle Program Payload Bay Payload User's Guide. National Aeronautics and Space Administration, 2000. 255 p.

6. Проектирование самолётов / С. М. Егер, В. Ф. Мишин, Н. К. Лисейцев и др. М. : Машиностроение, 1983. 616 с.

7. Spencer B. Jr., Fox C. H. Jr., Huffman J. K. A Study to Determine Methods of Improving the Subsonic Performance of A Proposed Personnel Launch System. Virginia : NASA Technical Memorandum, 1995. 82 p.

8. Лукашевич В. П., Афанасьев И. Б. Космические крылья. М. : ЛенТа Странствий, 2009. 496 с.

9. Буран РУ [Электронный ресурс]. URL: http://buran.ru/htm/spiral.htm (дата обращения 15.02.2024).

10. Параметрический анализ анизогридного корпуса космического аппарата для очистки орбиты от космического мусора / И. Д. Белоновская, В. В. Кольга, И. С. Ярков, Е. А. Яркова // Сибирский аэрокосмический журнал. 2021. Т. 22, № 1. С. 94–105. Doi: 10.31772/2712-8970-2021-22-1-94-105.

11. Государственный космический научно-производственный центр имени М. В. Хруничева [Электронный ресурс]. URL: http://www.khrunichev.ru/main.php?id=300 (дата обращения 16.02.2024).

12. Железнякова А. Л. Компьютерное моделирование спуска орбитальной ступени космической системы Space Shuttle в плотных слоях атмосферы Земли // Физико-химическая кинетика в газовой динамике. 2017. Т. 18, вып. 2 [Электронный ресурс]. URL: http://chemphys.edu.ru/issues/2017-18-2/articles/716/.

13. Грифитс Дж. Научные методы исследования осадочных пород / пер. с англ. Э. А. Еганова, А. В. Ильина и Г. И. Ратниковой. М. : Мир, 1971. 422 с.

14. ГОСТ 4401–81. Атмосфера стандартная. Параметры. М. : Стандартинформ, 2004. 181 с.

15. Остославский И. В., Стражева И. В. Динамика полёта траектории летательных аппаратов. М. : Машиностроение, 1969. 500 с.

References

1. Solovev V. A. [Development of the manned space flight program at the Russian Space Station]. *XLVIII Akademicheskie chteniya po kosmonavtike posvyashchennye pamyati akademika S. P. Koroleva i drugikh vydayushchikhsya otechestvennykh uchenykh – pionerov osvoeniya kosmicheskogo prostranstva* [XLVIII Academic readings on cosmonautics are dedicated to the memory of Academician S. P. Korolev and other prominent Russian scientists – pioneers of space exploration]. Moscow, 2024 (In Russ.).

2. Buran RU. Available at: http://buran.ru/htm/maxmain.htm (accessed 13.02.2024).

3. Arthur C. Grantz. X-37B Orbital Test Vehicle and Derivatives. *AIAA SPACE 2011 Conference & Exposition*. California, 2011, 14 p.

4. Lox U. *Dinamika i termodinamika spuska v atmosfere planet* [Dynamics and thermodynamics of descent in the atmosphere of planets]. Moscow, Mir Publ., 1966, 276 p.

5. Lyndon B. J. Space Shuttle Program Payload Bay Payload User's Guide. National Aeronautics and Space Administration, 2000. 255 p.

6. Eger S. M., Mishin V. F., Liseytsev N. K and other. *Proektirovanie samoletov* [Aircraft design]. Moscow, Mashinostroenie Publ, 1983, 616 p.

7. Spencer B. Jr., Fox C. H. Jr., Huffman J. K. A Study to Determine Methods of Improving the Subsonic Performance of A Proposed Personnel Launch System B. Virginia: NASA Technical Memorandum, 1995, 82 p.

8. Lukashevich V. P., Afanasev I. B. *Kosmicheskie krylya* [Space Wings]. Moscow, LenTa Stranstviy, 2009, 496 p.

9. Buran RU. Available at: http://buran.ru/htm/spiral.htm (accessed 15.02.2024).

10. Belonovskaya I. D., Kolga V. V., Yarkov I. S., Yarkova E. A. [Parametric analysis of the anisogrid body of the spacecraft for cleaning the orbit of space debris]. *Siberian Aerospace Journal*. 2021, Vol. 22, No. 1, P. 94–105. Doi: 10.31772/2712-8970-2021-22-1-94-105.

11. Khrunichev state research and production space center. Available at: http://www.khrunichev.ru/main.php?id=300 (accessed: 16.02.2024).

12. Zheleznyakova A. L. [Computer simulation of the descent of the orbital stage of the Space Shuttle space system in the dense layers of the Earth's atmosphere]. *Fiziko-khimicheskaya kinetika v gazovoy dinamike*. 2017, Vol. 18, No. 2. Available at: http://chemphys.edu.ru/issues/2017-18-2/articles/716/ (In Russ).

13. Griffiths J. *Nauchnye metody issledovaniya osadochnykh porod* [Scientific Method in Analysis of Sediments]. Moscow, Mir Publ., 1971, 422 p.

14. *GOST 4401–81. Atmosfera standartnaya. Parametry* [Siandart atmosphere. Parameters]. Moscow, Standartinform Publ., 2004. 181 c.

15. Ostroslavskiy I. V., Strazheva I. V. *Dinamika poleta traektorii letatel'nykh apparatov* [Flight dynamics of the trajectory of aircraft]. Moscow, Mashinostroenie Publ., 1969, 500 p., ill.

Кольга Вадим Валентинович – доктор педагогических наук, кандидат технических наук, профессор, профессор кафедры летательных аппаратов; Сибирский государственный университет науки и технологий имени академика М. Ф. Решетнева. E-mail: kolgavv@yandex.ru.

Рундау Никита Сергеевич – студент; Сибирский государственный университет науки и технологий имени академика М. Ф. Решетнёва. E-mail: nik290200@mail.ru.

Kolga Vadim Valentinovich – Dr. Sc., professor, Cand. Sc., Professor of Department of Aircraft; Reshetnev Siberian State University of Science and Technology. E-mail: kolgavv@yandex.ru.

Rundau Nikita Sergeevich – student; Reshetnev Siberian State University of Science and Technology. E-mail: nik290200@mail.ru.